A 512-Channel Multi-Layer Polymer-Based Neural Probe Array

Kee Scholten, *Member, IEEE*, Christopher E. Larson, *Member, IEEE*, Huijing Xu, *Member, IEEE*, Dong Song, *Senior Member, IEEE*, and Ellis Meng, *Fellow, IEEE*

***Abstract*— We present for the first time the design, fabrication, and preliminary bench-top characterization of a high-density, polymer-based penetrating microelectrode array, developed for chronic, large-scale recording in the cortices and hippocampi of behaving rats. We present two architectures for these targeted brain regions, both featuring 512 Pt recording electrodes patterned front-and-back on micromachined eight-shank arrays of thin-film Parylene C. These devices represent an order of magnitude improvement in both number and density of recording electrodes compared with prior work on polymer-based microelectrode arrays. We present enabling advances in polymer micro-machining related to lithographic resolution and a new method for back-side patterning of electrodes. *In vitro* electrochemical data verifies suitable electrode function and surface properties. Finally, we describe next steps toward the implementation of these arrays in chronic, large-scale recording studies in free-moving animal models. [2020-0109]**

***Index Terms*— Microelectrode array, brain machine interfaces, neural probe, Parylene, bioMEMS.**

I. Introduction

SILICON microelectrode arrays (MEAs) featuring hundreds to thousands of recording sites represent the state-of-the-art in penetrating brain-machine interfaces [1], [2] however the significant mismatch between the mechanical properties of stiff silicon and soft brain tissue (Young's modulus $>$ 150 GPa and $\sim$1 kPa, respectively) presents a tremendous obstacle for chronic recording. Strain-induced tissue damage at the tissue-implant interface can occur from normal micromotion of the brain, exacerbating the chronic immune response and leading to astrogliosis, scar encapsulation, neuronal migration and even neuronal death [3]–[5]. In both formal and anecdotal accounts, silicon MEAs are often associated with a drop in recording performance and prominent immune response following 2-4 weeks post implantation [6]–[9].

Polymer-based MEAs have drawn increasing interest as a possible solution. Polymer MEAs can be up to 100$\times$ softer than their silicon counterparts and offer additional benefits like optical transparency, flexibility, and material biocompatibility. However, polymer MEAs have lagged far behind silicon devices in terms of electrode density and count, typically featuring just tens of electrodes across an array. Recent breakthroughs have demonstrated the first large-scale polymer MEAs, with high resolution micromachining of solvent-cast polymers (SU-8, polyimide) [10]–[12]. However, even these devices are limited to just 32 electrodes per penetrating shank, compared to hundreds for the state-of-the-art in silicon. Improvements in microlithographic processes on polymer materials is required to achieve the resolution required to close this gap.

Here we present a new approach for high-channel count polymer MEAs, a dual-sided array built using vapor deposited Parylene C. Our Parylene MEAs (Fig. 1) possess the highest electrode count per probe (64) of any polymer neural probe described to date. In this work we describe the design, fabrication, and initial testing of prototypes intended for both cortical and hippocampal chronic recording in rat models.

II. Methods

A. Design

The overall design of the 512-channel Parylene C MEA builds upon prior Parylene MEA architectures [13]–[15] and consists of 8 polymer shanks, each supporting 64 platinum electrodes (32 each on the front and back). Two layouts are presented here (Fig. 2), one with 2 mm long shanks for cortical recording in rat models, and one with 5.5 mm long shanks for hippocampal recording. Shanks are tapered from 230 μm down to 140 μm wide at the tip. The 8 shanks connect into a single 12 mm long ribbon cable which terminates in a series of contact pads for connection to an electrode interface board by way of a zero-insertion force (ZIF) connector.

Each electrode is 30 μm in diameter, with the outer 5 μm insulated with Parylene C, such that the exposed electrode is 20 μm in diameter. Each electrode is individually addressed by a 2 μm wide platinum trace patterned on the same layer as the corresponding electrode. No vias were used for the construction of these devices. Traces are spaced just 2 μm apart to minimize shank width.

The devices are fabricated using multiple layers of vapor deposited Parylene C and patterned thin-film platinum. The base layer is 2 μm of Parylene C, followed by the bottom metal layer (containing back electrodes, traces and contact

Manuscript received April 30, 2020; accepted May 24, 2020. Date of publication June 11, 2020; date of current version October 7, 2020. This work was supported in part by the National Institutes of Health through the BRAIN Initiative under Award U01 NS099703 and in part by the University of Southern California Provost Fellowship. Subject Editor R. Sochol. *(Corresponding author: Ellis Meng.)*

The authors are with the Department of Biomedical Engineering, University of Southern California, Los Angeles, CA 90089-1111 USA (e-mail: ellis.meng@usc.edu).

Color versions of one or more of the figures in this article are available online at http://ieeexplore.ieee.org.

Digital Object Identifier 10.1109/JMEMS.2020.2999550

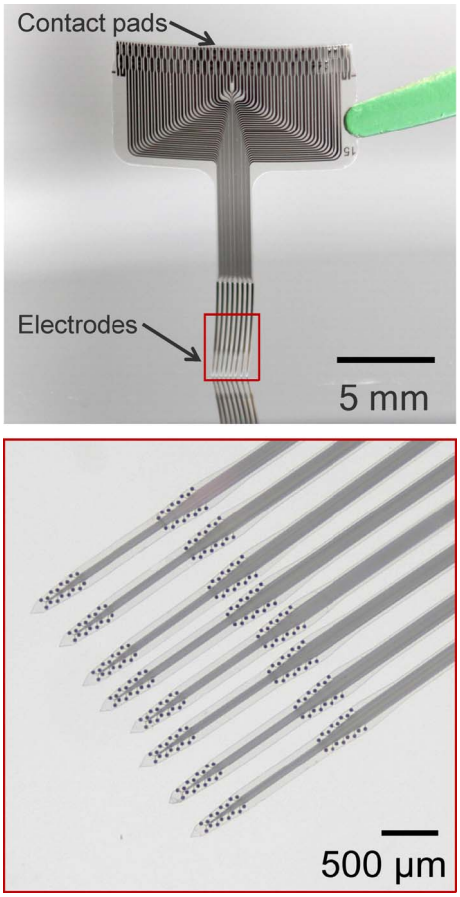

Fig. 1. Photograph of a large-scale, polymer-based brain-machine interface designed to record from rat hippocampi. Magnified view (bottom) shows 256 visible electrodes matched by an equal number on the backside.

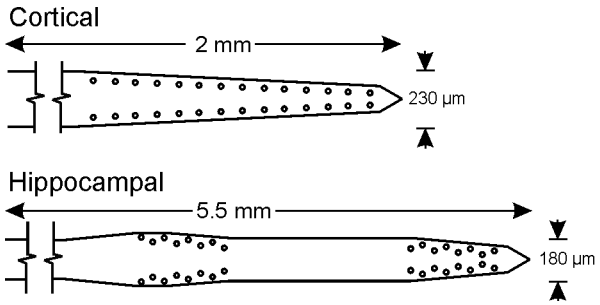

Fig. 2. Electrode layout and relevant dimensions of the cortical and hippocampal probe designs. The hippocampal probe electrodes are conformally arranged to match the location of cell body layers.

pads, 200 nm thick). This layer is insulated in 8 μm of Parylene C, which also serves as the support for the top metal layer (200 nm). The top metal layer is insulated in a final 10 μm of Parylene C. The total thickness is approximately 20 μm.

For the purposes of the experiments described here, only 64 electrodes of the 512 total were addressable through the electrode interface board, although all electrodes are inferred to be functional. Future devices will integrate digital multiplexing to allow connection to all electrodes without the need for 512 analog connections exiting the board.

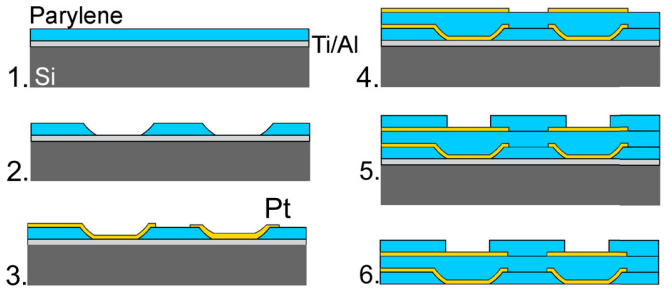

Fig. 3. Cross-section view of polymer MEA fabrication process flow: (1) Parylene was deposited on Al release layer. (2) O_2 etch created openings for backside electrodes. (3) Electrodes, traces and contacts were deposited and patterned. (4) Parylene was deposited followed by a second patterned metal layer (5) Frontside electrodes were etched open with O_2 plasma. (6) Al layer was dissolved and devices released.

B. Fabrication

MEAs were fabricated using a low-temperature, batch-scale, multi-layer process summarized in Fig. 3. The final devices consist of two metal layers sandwiched and insulated between three layers of Parylene C. Processing was performed on 4-inch diameter silicon carrier wafers, which were coated in a 100 nm Al sacrificial layer with a 10 nm Ti adhesion layer. The Al layer was chemically roughened with an 8 minute etch in CR-7 (Transene Company, Danvers MA) to maintain adhesion of the base Parylene C layer during subsequent processing. The base Parylene C layer was deposited by room temperature chemical vapor deposition to a thickness of 2 μm. An isotropic O_2 reactive ion etch, masked by photopatterned P4620 photoresist (Integrated Micro Materials, Argyle TX), was used to open holes in this base layer for the backside electrodes. Next, Pt was deposited and patterned, containing the 256 back electrodes and associated traces and contact pads. The metal layer pattern was created using a lift-off photoresist mask (AZ5214, Integrated Micro Materials, Argyle TX), having a resolution of 2 μm. Then Pt was deposited by e-beam evaporation to 200 nm total thickness, using four sequential deposition steps of 50 nm with 30-minute cooling pauses in between to reduce thermal stress. Next, an 8 μm conformal insulating layer of Parylene C was deposited over this first Pt layer. A second layer of Pt electrodes, traces, and contact pads was deposited and patterned in the same manner. This layer was coated in a final 10 μm of Parylene C. Finally, the Parylene C over the top electrodes was removed using a deep reactive O_2 ion etch across a P4620 photoresist mask, and the outline of the MEAs was 'cut-out' using a second etch step performed in the same manner.

Devices were released by dissolving the Al adhesion layer in warm tetramethylammonium hydroxide. In a post-processing step, individual devices were annealed at 200 °C for 48 hours under vacuum, while pressed flat between two Teflon sheets. This step served both to reduce curvature in the final device and to reduce pore sizes in the semi-crystalline Parylene C.

C. Characterization and Analysis

Electrode properties and end-to-end continuity were evaluated using cyclic voltammetry (CV) and electrochemical

impedance spectroscopy (EIS). MEAs were connected to a printed-circuit board using a 71 channel ZIF connector (FH43B-71S-0.2SHW, Hirose Electric Co, Tokyo) with a ∼100 μm thick polyethylene terephthalate film backer for structural support. The test board connected each of the 64 addressable electrodes to an array of header pins, which were connected to a potentiostat (Reference 600, Gamry Instruments, Philadelphia) for testing. CV was performed in 0.05 M H_2SO_4 in the potential range of −0.2–1.2 V versus an Ag/AgCl reference and large Pt counter electrode. The solution was purged with N_2 prior to and during the CV. Scan rate was 250 mV/s for 30 cycles. EIS was performed in 1× phosphate-buffered saline (PBS) following CV cycling, also using Ag/AgCl and Pt as the reference and counter, respectively. Impedance was measured across 1 Hz–1 MHz.

Trace-to-trace capacitance was estimated using finite element modeling in LISA software. Parylene C was assumed to be perfectly conformal in the intercalary space between traces, with a relative permittivity coefficient of 3.1, taken from literature values [16]. Attempts to measure capacitance with available equipment (Keysight E4980AL) confirmed values at or below a noise floor of ∼1 pF.

III. Results

Several important observations were recorded during initial attempts to fabricate the MEAs. Unlike prior Parylene MEAs, a sacrificial Al layer was required to prevent the base Parylene C layer from lifting off from the carrier wafer during processing as a result of etched openings in the base layer for the back electrodes. Parylene C exhibited very high adhesion to sputtered Al, but almost no adhesion to evaporated Al, a result we attribute to differences in surface roughness. Treating the evaporated Al with CR-7 (measured etch rate ∼6 nm/min) introduced the desired adhesion. The sacrificial layer also proved necessary during the first Pt deposition step. When fabrication was attempted without the adhesion layer, the base Parylene C (2 μm) wrinkled following Pt evaporation, presumably from thermal stress. Presence of the Al eliminated this effect. Achieving the 2 μm resolution lift-off mask was nontrivial and required tight control of all process parameters and strong Parylene-photoresist adhesion (Fig. 4). Parylene C is not compatible with typical surface treatments such as hexamethyldisilazane (HMDS). Instead, prior to photoresist spinning, wafers were baked for 30 minutes at 60 °C and 1/2 atm under a stream of dry N_2 to remove moisture without oxidizing the polymer film. Following this treatment, lithography was successful and repeatable, suggesting UV lithography on Parylene C may be pushed to the optical limit.

Completed MEAs were functional and robust. The polymer shanks were highly compliant despite the high density of metal traces. Trace-to-trace capacitance was estimated as ∼0.2 pF from finite element analysis and did not measurably increase electrode impedance. Electrical continuity of the backside electrodes was confirmed with EIS and CV; Fig. 5 shows representative measurement data of an electrode following cyclic voltammetric cycling. Impedance of the 20 μm electrodes was ∼1 MΩ at 1 kHz. This is consistent with impedance values

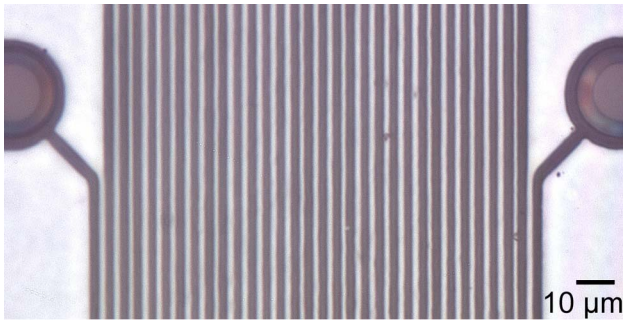

Fig. 4. Micrograph of patterned Pt traces and electrodes on Parylene substrate with 2 μm pitch/width. Exposed electrode diameter is 20 μm.

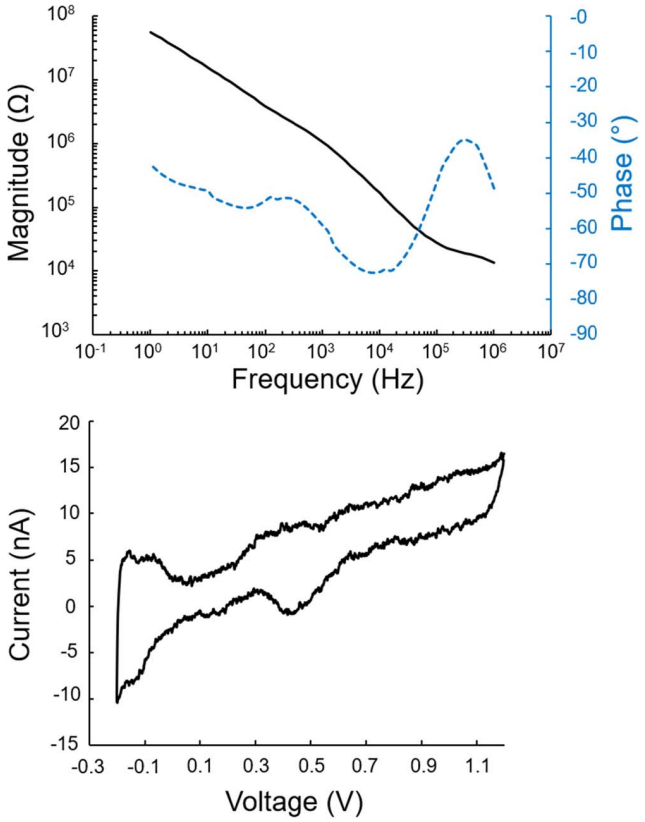

Fig. 5. Data characterizing the impedance and surface properties of the Pt electrodes. (Top) EIS data showing magnitude (left) and phase (right) of a representative electrode in 1 × PBS. (Bottom) CV data of the same electrode, after 30 cycles, showing characteristic hydrogen absorption/desorption and oxide formation and reduction.

from larger electrodes (30 μm diameter; 0.5-0.6 MΩ at 1 kHz) produced on a prior Parylene C-based device [14].

IV. Discussion

The fine microlithographic resolution achieved here, combined with the multi-layer design, increased electrode density while minimizing width of each flexible polymer shank. Smaller pitch and spacing for microtraces on a polymer MEA have been reported [12], [17], but using electron-beam lithography, which is a low throughput, serial process that substantially increases fabrication cost. UV lithography was

achieved at batch-scale and is amenable to mass production with lower costs and higher yield.

EIS and CV measurements confirmed the required electrochemical properties for neural recording and validated our approach for via-less front and back electrodes. Impedance values were consistent with the exposed electrode diameter, suggesting the dominant driver of impedance was electrode surface area. As trace size for neural interfaces continues to shrink, there is a risk that trace impedance or capacitive coupling will drive up impedance, and therefore signal noise. However, the results here suggest there is room for further miniaturization, allowing polymer MEAs to approach the channel density of silicon devices. The impedance values of these electrodes (1 MΩ at 1 kHz) may impede high quality recordings but can be coated with a high surface area platinum-iridium alloy [18], an approach we have demonstrated with similar Parylene C MEAs in an unpublished study.

The next steps are to obtain successful electrophysiological recordings in rats using these MEAs and from two different brain regions. Implantation of long, flexible polymer probes can be challenging, as they are likely to buckle during insertion. In prior work we demonstrated a simple insertion method with similar Parylene C MEAs [14] that does not require use of an introducer tool or stiffening agent. Instead, the probe shanks will be partially encased by a brace made of polyethylene glycol, leaving a short section of the tips exposed. By reducing the effective length of the probes in this way, the buckling force increases significantly, allowing the bare probes to be gradually inserted as the remaining brace dissolves in saline. This allows for insertion without introducing any material but the Parylene C probes into the brain.

The most significant challenge in developing this technology is addressing all 512 electrodes. Current ZIF connectors do not extend to this size, and so the same connection scheme (common to polymer MEAs) would require a split ribbon cable and multiple connectors. Analog output connectors similarly are not available with 512 channels, in a size suitable for free-moving animal experiments. The most plausible path forward will require integration of multiplexing ASICs directly into the ribbon cable. We recently developed a novel ultrasonic bonding method for direct packaging of ASIC to Parylene C devices [19]. This approach will allow us to forgo both the need for a ZIF connector and analog output, while reducing the density of contact pads.

With respect to application, the high-density polymer-based neural probe described here is developed in the context of performing animal studies on long-term synaptic plasticities, which requires high-quality, stable recordings of unitary activities for long periods of time [20]. Such a probe also has the potential to be used as a therapeutic device in clinical applications such as closed-loop deep brain stimulation (DBS) [21], [22] and cortical prostheses [23], [24] for treating neurological disorders, where high biocompatibility and fine spatio-temporal resolution become critical. One important future direction is to add stimulation capability to the polymer-based neural probes to achieve bi-directional communication between the device and the neural tissue.

V. Conclusion

A Parylene C based MEA for cortical and subcortical neural recording in free-moving rats was fabricated, bench-top evaluated and tested. A novel microfabrication approach was designed to allow for high-resolution patterning on the flexible polymer base that enables front and back patterning of electrodes on either side of a 140-230 μm wide Parylene C probe shank. A key fabrication improvement was the addition of a chemically roughened Al adhesion layer, that ensured the Parylene C did not wrinkle or lift-off from the carrier wafer and could be easily removed at the end of fabrication. The devices presented here represent the highest channel count per shank among polymer MEAs and among the highest total channel count for a polymer MEA. The flexible, soft composition of the probe array is expected to allow for chronic recording in free-moving animals by mitigating tissue trauma. The designs and method presented here pave the way for polymer MEAs to match channel density of the state-of-the-art in silicon devices.

Acknowledgment

The authors would like to thank Dr. Donghai Zhu and the USC Keck Photonics Cleanroom for assistance in device fabrication, and Xuechun Wang for assistance in electrochemical measurements.

References

[1] J. J. Jun *et al.*, "Fully integrated silicon probes for high-density recording of neural activity," *Nature*, vol. 551, no. 7679, pp. 232–236, Nov. 2017, doi: 10.1038/nature24636.

[2] G. Rios, E. V. Lubenov, D. Chi, M. L. Roukes, and A. G. Siapas, "Nanofabricated neural probes for dense 3-D recordings of brain activity," *Nano Lett.*, vol. 16, no. 11, pp. 6857–6862, Nov. 2016, doi: 10.1021/acs.nanolett.6b02673.

[3] H. C. Lee *et al.*, "Histological evaluation of flexible neural implants; flexibility limit for reducing the tissue response?" *J. Neural Eng.*, vol. 14, no. 3, p. 36026, 2017.

[4] R. Biran, D. C. Martin, and P. A. Tresco, "Neuronal cell loss accompanies the brain tissue response to chronically implanted silicon microelectrode arrays," *Exp. Neurol.*, vol. 195, no. 1, pp. 115–126, Sep. 2005, doi: 10.1016/j.expneurol.2005.04.020.

[5] R. Biran, D. C. Martin, and P. A. Tresco, "The brain tissue response to implanted silicon microelectrode arrays is increased when the device is tethered to the skull," *J. Biomed. Mater. Res. A*, vol. 82A, no. 1, pp. 169–178, Jul. 2007, doi: 10.1002/jbm.a.31138.

[6] N. F. Nolta, M. B. Christensen, P. D. Crane, J. L. Skousen, and P. A. Tresco, "BBB leakage, astrogliosis, and tissue loss correlate with silicon microelectrode array recording performance," *Biomaterials*, vol. 53, pp. 753–762, Jun. 2015, doi: 10.1016/j.biomaterials.2015.02.081.

[7] M. P. Ward, P. Rajdev, C. Ellison, and P. P. Irazoqui, "Toward a comparison of microelectrodes for acute and chronic recordings," *Brain Res.*, vol. 1282, pp. 183–200, Jul. 2009, doi: 10.1016/j.brainres.2009.05.052.

[8] H. C. Lee, J. Gaire, B. Roysam, and K. J. Otto, "Placing sites on the edge of planar silicon microelectrodes enhances chronic recording functionality," *IEEE Trans. Biomed. Eng.*, vol. 65, no. 6, pp. 1245–1255, Jun. 2018, doi: 10.1109/TBME.2017.2715811.

[9] R. J. Vetter, J. C. Williams, J. F. Hetke, E. A. Nunamaker, and D. R. Kipke, "Chronic neural recording using silicon-substrate microelectrode arrays implanted in cerebral cortex," *IEEE Trans. Biomed. Eng.*, vol. 51, no. 6, pp. 896–904, Jun. 2004, doi: 10.1109/TBME.2004.826680.

[10] E. Musk and Neuralink, "An integrated brain-machine interface platform with thousands of channels," *J. Med. Internet Res.*, vol. 21, no. 10, Oct. 2019, Art. no. e16194, doi: 10.2196/16194.

[11] J. E. Chung *et al.*, "High-density, long-lasting, and multi-region electrophysiological recordings using polymer electrode arrays," *Neuron*, vol. 101, no. 1, pp. 21.e5–31.e5, Jan. 2019, doi: 10.1016/j.neuron.2018.11.002.

[12] X. Wei *et al.*, "Nanofabricated ultraflexible electrode arrays for high-density intracortical recording," *Adv. Sci.*, vol. 5, no. 6, Jun. 2018, Art. no. 1700625, doi: 10.1002/advs.201700625.
[13] A. W. Hirschberg, H. Xu, K. Scholien, T. W. Berger, D. Song, and E. Meng, "Development of an anatomically conformal parylene neural probe array for multi-region hippocampal recordings," in *Proc. IEEE 30th Int. Conf. Micro Electro Mech. Syst. (MEMS)*, Jan. 2017, pp. 129–132, doi: 10.1109/MEMSYS.2017.7863357.
[14] H. Xu, A. W. Hirschberg, K. Scholten, T. W. Berger, D. Song, and E. Meng, "Acute *in vivo* testing of a conformal polymer microelectrode array for multi-region hippocampal recordings," *J. Neural Eng.*, vol. 15, no. 1, p. 16017, 2018.
[15] B. J. Kim *et al.*, "3D parylene sheath neural probe for chronic recordings," *J. Neural Eng.*, vol. 10, no. 4, May 2013, Art. no. 045002, doi: 10.1088/1741-2560/10/4/045002.
[16] (2016). *SCS Parylene Properties*. Accessed: Apr. 28, 2020. [Online]. Available: https://scscoatings.com/wp-content/uploads/2017/09/02-SCS-Parylene-Properties-1016.pdf
[17] K. Scholten and E. Meng, "Electron-beam lithography for polymer bioMEMS with submicron features," *Microsyst. Nanoeng.*, vol. 2, no. 1, pp. 1–7, Nov. 2016, doi: 10.1038/micronano.2016.53.
[18] A. Petrossians, J. J. Whalen, J. D. Weiland, and F. Mansfeld, "Surface modification of neural stimulating/recording electrodes with high surface area platinum-iridium alloy coatings," in *Proc. Annu. Int. Conf. IEEE Eng. Med. Biol. Soc. (EMBS)*, Aug. 2011, pp. 3001–3004, doi: 10.1109/IEMBS.2011.6090823.
[19] J. J. Yoo and E. Meng, "Fine-pitch bonding methods for integrating ASICs with flexible polymer MEMS," in *Proc. 20th Int. Conf. Solid-State Sens., Actuators Microsyst. Eurosensors (TRANSDUCERS EUROSENSORS)*, Jun. 2019, pp. 1623–1626, doi: 10.1109/TRANSDUCERS.2019.8808219.
[20] D. Song *et al.*, "Identification of functional synaptic plasticity from spiking activities using nonlinear dynamical modeling," *J. Neurosci. Methods*, vol. 244, pp. 123–135, Apr. 2015, doi: 10.1016/j.jneumeth.2014.09.023.
[21] J. S. Perlmutter and J. W. Mink, "Deep brain stimulation," *Annu. Rev. Neurosci.*, vol. 29, no. 1, pp. 229–257, Jul. 2006, doi: 10.1146/annurev.neuro.29.051605.112824.
[22] A. Ramirez-Zamora *et al.*, "Evolving applications, technological challenges and future opportunities in neuromodulation: Proceedings of the fifth annual deep brain stimulation think tank," *Frontiers Neurosci.*, vol. 11, p. 734, Jan. 2018, doi: 10.3389/fnins.2017.00734.
[23] D. Song, B. S. Robinson, R. E. Hampson, V. Z. Marmarelis, S. A. Deadwyler, and T. W. Berger, "Sparse large-scale nonlinear dynamical modeling of human hippocampus for memory prostheses," *IEEE Trans. Neural Syst. Rehabil. Eng.*, vol. 26, no. 2, pp. 272–280, Feb. 2018, doi: 10.1109/TNSRE.2016.2604423.
[24] R. E. Hampson *et al.*, "Developing a hippocampal neural prosthetic to facilitate human memory encoding and recall," *J. Neural Eng.*, vol. 15, no. 3, p. 36014, 2018.

Kee Scholten (Member, IEEE) was born in Adelaide, SA, Australia, in 1987. He received the B.S. degree in applied physics from the California Institute of Technology (Caltech) in 2009 and the Ph.D. degree in applied physics from the University of Michigan in 2014. He is currently the Director of the Polymer Implantable Electrode Foundry, University of Southern California, Los Angeles. His research interests include implantable and wearable microsensors, ubiquitous chemical and biomedical sensing, and flexible MEMS and nanoelectronics.

Christopher E. Larson (Member, IEEE) was born in St. Paul, MN, USA, in 1987. He received the B.M. degree in music composition from Biola University in 2009 and the B.S. degree in biomedical engineering from the University of Southern California (USC) in 2015, where he is currently pursuing the Ph.D. degree with the Biomedical Microsystems Laboratory, developing polymer MEMS-based neural interfaces and other implantable medical devices.

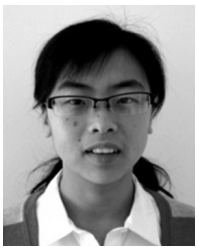

Huijing Xu (Member, IEEE) received the B.S. degree in biomedical engineering from Shanghai Jiao Tong University and the Ph.D. degree in biomedical engineering from the University of Southern California in 2019. She continued studying biomedical engineering at USC and developed her interests in neural engineering and cortical prostheses. In 2011, she joined the Center for Neural Engineering (CNE), where she works under the direction of Prof. T. W. Berger and Prof. D. Song. Her research focuses on the development of novel neural interfacing techniques and the understanding of the function of the hippocampus in memory processing. In specific, she works on the design and development of conformal multi-electrode arrays that can record neural activities from multiple sub-regions of the hippocampus simultaneously from behaving animals and to conduct behavioral experiments to study the information transformation within the hippocampus tri-synaptic circuit.

Dong Song (Senior Member, IEEE) received the B.S. degree in biophysics from the University of Science and Technology of China in 1994 and the Ph.D. degree in biomedical engineering from the University of Southern California in 2004. He became a Research Assistant Professor and a Research Associate Professor at the Department of Biomedical Engineering, University of Southern California (USC), in 2006 and 2013, respectively. He is the Co-Director of the Center for Neural Engineering, USC. His research is supported by the DARPA, NSF, and NIH. His research interests include nonlinear dynamical modeling of the nervous system, hippocampal memory prosthesis, neural interface technologies, and the development of novel modeling strategies incorporating both statistical and mechanistic modeling methods. He is a member of the American Statistical Association, the Biomedical Engineering Society, the Society for Neuroscience, the Society for Brain Mapping and Therapeutics, Organization for Computational Neurosciences, and the National Academy of Inventors. He received the James H. Zumberge Individual Award from the USC in 2008, the Outstanding Paper Award of the IEEE TRANSACTIONS ON NEURAL SYSTEMS AND REHABILITATION ENGINEERING in 2013, and the Society for Brain Mapping and Therapeutics Young Investigator Award in 2018.

Ellis Meng (Fellow, IEEE) received the B.S. degree in engineering and applied science and the M.S. and Ph.D. degrees in electrical engineering from the California Institute of Technology (Caltech), Pasadena, in 1997, 1998, and 2003, respectively. She is a Professor of Biomedical Engineering and the Vice Dean of Technology Innovation and Entrepreneurship with the Viterbi School of Engineering, University of Southern California, Los Angeles. She also holds a joint appointment with the Ming Hsieh Department of Electrical and Computer Engineering. Her research interests include bioMEMS, implantable biomedical microdevices, microfluidics, multimodality integrated microsystems, and packaging. She is a fellow of the ASME, BMES, AIMBE, and NAI. She held the Viterbi Early Career Chair and the Gabilan Distinguished Professorship in Science and Engineering, and was the Department Chair from 2015 to 2018. Her honors include the NSF CAREER and Wallace H. Coulter Foundation Early Career Translational Research Awards, the 2009 TR35 Young Innovator under 35, the ASEE Curtis W. McGraw Research Award, the 2018 IEEE Engineering in Medicine and Biology Society Technical Achievement Award, and the 2019 IEEE Sensors Council Technical Achievement Award.